IDA

INSTITUTE FOR DEFENSE ANALYSES

Antenna Measures of Merit for Ultra-Wide Synthetic Aperture Radar

Elizabeth Li Ayers
James M. Ralston
Institute for Defense Analyses

R. Paul Maloney
Philip G. Tomlinson
Decision-Science Applications, Inc.

John McCorkle
Army Research Laboratory

September 1998

Approved for public release;
distribution unlimited.

IDA Document D-2200

Log: H 98-002558

This work was conducted under contract DASW01 94 C 0054, Task Assignment A-155, for the Defense Advanced Research Projects Agency/ Information Systems Office. The publication of this IDA document does not indicate endorsement by the Department of Defense, nor should the contents be construed as reflecting the official position of that Agency.

PREFACE

This work was undertaken for the Defense Advanced Research Projects Agency under a task entitled "Counter Camouflage Concealment and Deception (CC&D) Systems Studies" as part of the program to develop ultra-wideband radar technology for detecting hostile targets that may be covered, concealed, or camouflaged. This document was originally presented at the IEEE 1998 National Radar Conference held in Dallas, Texas, 12–13 May 1998, and is published in the conference proceedings.

ANTENNA MEASURES OF MERIT FOR ULTRA-WIDE SYNTHETIC APERTURE RADAR*+

Elizabeth Li Ayers, James M. Ralston
The Institute for Defense Analyses, Alexandria, Virginia

R. Paul Maloney, Philip G. Tomlinson
Decision-Science Applications, Inc., Arlington, Virginia

John McCorkle
Army Research Laboratory, Adelphi, Maryland

ABSTRACT

This paper addresses the issue of how to characterize an antenna's performance in a SAR system—particularly in ultra-wide-bandwidth and/or ultra-wide-angle (UWB/A) SAR—based on simple gain-magnitude versus frequency and angle measurements provided in data sheets. We present eight measures of merit. As illustrative examples, we compare an ideal mathematical model to measurements of an actual antenna designed to perform UWB/A SAR over up to 65-degree integration angles and over a 150- to 550-MHz frequency band.

1.0 INTRODUCTION

Recent years have seen the development of airborne SAR systems in the VHF/UHF frequency range that achieve high resolution through a combination of wide-bandwidth and wide-angle target illumination (hereinafter called ultrawide SAR). The specification and selection of antenna components for these SARs has tended to rely on the same methods developed for narrowband SAR in the microwave regime. The results, however, are often less than satisfactory because antenna designers have had no clear mapping between antenna pattern tradeoffs and UWB/A SAR image quality. Many of the accepted antenna measures-of-merit (MoM), which can be used to predict performance of narrow-band SAR systems, do not necessarily apply to ultrawide SAR. For example, when the bandwidth approaches 100%, the beamwidth, gain, efficiency, phase-center, etc., all vary significantly with frequency. Figure 1 illustrates the issue.

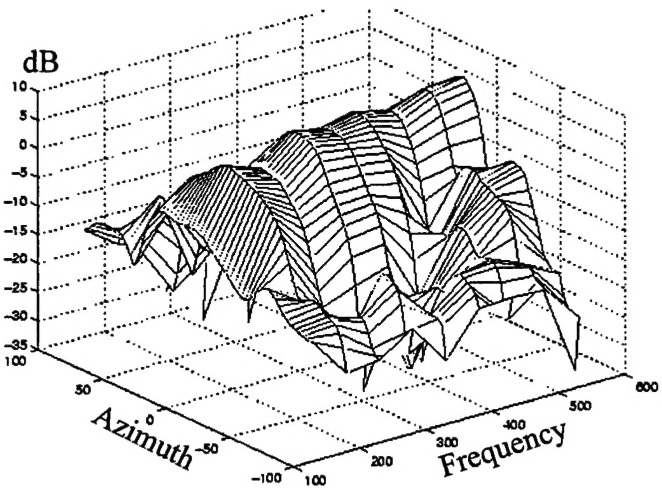

Figure 1. Pattern Of BATC Circles Array, HH-Polarization. Azimuth Refers To A Great-Circle Cut At 30 Degrees Depression From The SAR Wing Plane

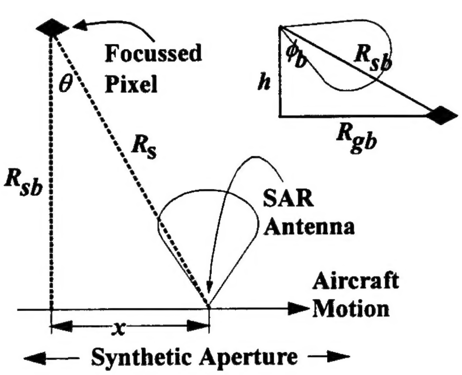

Figure 2. SAR Geometry Notation

Shown is the Ball Aerospace & Technologies Corporation (BATC) "circles-array" antenna pattern as a function of azimuth angle and frequency. Conventional narrow-band SAR analysis would reduce the detail of this plot to a single beamwidth and a single gain that is assumed to apply over the entire bandwidth. Antennas to be used in ultrawide SAR have the following conflicting requirements:

* Presented at the IEEE 1998 National Radar Conference, Dallas, Tx. 12-13 May 1998
+ Research supported by the Defense Advanced Research Projects Agency

- An adequate level of real-aperture gain throughout the coherent aperture. This should ensure sufficient signal energy from individual pixels to provide adequate signal- or clutter-to-noise ratios.
- Adequate beamwidth or scene angle at each frequency to give the required resolution.
- Controlled/minimized response in extraneous directions. This is needed to minimize the slow-time Doppler spectrum, wrong-side ambiguities, sky noise, and radio-frequency interference (RFI) to the extent practicable.
- A "well-behaved" impulse response in angle and frequency. Excessive variation in gain and phase versus angle and frequency can lead to excessive sidelobes or require equalization that will degrade signal-to-noise ratio.
- Adequate polarimetric purity over that beamwidth to give the required isolation in the images.

With the benefit of digital processing, it is possible to achieve good imaging performance with what would be considered, by traditional measures, unacceptable antenna patterns. Digital processing (inverse filtering) as described by Ertin et al [1] can relieve some of the burden of ultrawide SAR antenna design. But such processing implies a mismatch loss that must be considered, since angles and/or frequencies with low gain must be boosted at the expense of increased noise. By assuming that phase variations are digitally corrected, we derive quantitative formulas for predicting antenna performance in ultrawide SAR based solely on gain-magnitude versus frequency and angle. Framing the metrics in this fashion allows simple tables provided by antenna manufacturers to be used to compute the metrics. The metrics allows us to evaluate the antenna in terms of its impact upon image quality, including resolution, S/N, and ambiguities. We have analyzed measured and simulated (idealized) patterns, under the criteria derived. The results, which directly relate to ultrawide SAR system performance, can be used to guide future antenna specification and design efforts.

2.0 ANTENNA IMPACT ON SYSTEM SENSITIVITY

In this paper, the SAR is assumed to be operating in the typical side-looking straight line flight path mode. Consider the motion of the antenna during the coherent processing aperture shown in Figure 2. Here, R_{sb} is the slant range at broadside, and R_s and θ are the time-varying slant range and squint angle to a test pixel in the scene. Let ϕ_b be the elevation angle at broadside, measured from nadir, v be the aircraft speed, and h be the height. In this section, we assume that matched-filter processing applies. In this case, total signal energy is an appropriate measure of sensitivity. In a later section, we discuss the ramifications of other than matched-filter processing. During one coherent dwell, the total energy received from an object in the focused pixel is an integral of the received power density over both time in the aperture and the frequency spectrum of the waveform. This integral is shown in equation (1) where f_1 and f_2 are the upper and lower frequency limits, $|W_t(f)|^2$ is the normalized spectral power density (e.g. $1/(f_2-f_1)$) for a flat spectrum), $P_{av}|W_t(f)|^2$ is the average transmitted spectral power density, T is the integration time (i.e. time of flight to form the synthetic aperture), $|G(f,\theta,\phi)|$ is the antenna power gain, $R_s(t)$ is the slant range, and c is the speed of light.

$$E=\int_{f_1}^{f_2}\int_{-T/2}^{T/2}\frac{P_{av}|W_t(f)|^2|G(f,\theta(t),\phi(t))|^2(c/f)^2\sigma}{(4\pi)^3R_s^4(t)}dt\,df \tag{1}$$

Changing variables to integrate in angle space, and denoting a great circle cut by $G_{\phi_b}(f,\theta)$ yields:

$$dt=\frac{dx}{v}=\frac{R_{sb}\cdot d\theta}{v\cdot\cos^2(\theta)};\quad R_s(\theta)=\frac{R_{sb}}{\cos(\theta)};\quad \phi(\theta)=\cos^{-1}[\cos(\phi_b)\cos(\theta)];\quad G(f,\theta,\phi(\theta))=G_{\phi_b}(f,\theta)$$

$$E=\frac{P_{av}\cdot\sigma}{(4\pi)^3R_{sb}^3v}\cdot\Psi(\phi,\theta_1,\theta_2),\ \text{where}\ \Psi(\phi,\theta_1(f),\theta_2(f))=\int_{f_1}^{f_2}\int_{\theta_1(f)}^{\theta_2(f)}|W_t(f)|^2|G_\phi(f,\theta)|^2(c/f)^2\cos^2(\theta)d\theta\,df \tag{2}$$

The Ψ term contains the factors of interest to characterize the antenna. It has the dimension of square meters. It is a straightforward integral transformation of the two-dimensional (2D) great-circle measurements of antenna gain versus frequency and angle. And it can be computed from measurement points provided in data-sheets. The Ψ term can be thought of as an effective gain-aperture product that reflects both the real antenna aperture and the synthetic aperture. We will compute this gain aperture product over different angular regions to provide several metrics. If more data is available, each of these gain-aperture based metrics could be augmented to include a min, max, and average over the range of desired depression angles. Note that the integrand decays in the θ dimension, due not only to the $\cos^2(\theta)$ factor, but also to the antenna pattern. The first measure of antenna performance is

defined to be the effective gain-aperture product on the desired side. We use an integration angle of π to measure the potential of the antenna.

$$GA_d = \Psi(\phi_b, -\pi/2, \pi/2) \tag{3}$$

3.0 EFFECT OF ANTENNA UPON AMBIGUITY RATIOS

A major factor in choosing a SAR antenna is its capability to provide left-right isolation. That is, when the synthetic aperture is a straight line, image formation to the left and right sides is identical. The only isolation provided is that obtained by the antenna. The ratio of ambiguous to desired energy is given as a ratio of the gain-aperture products on the desired side versus the undesired side in equation (4).

$$A_{LR} = \frac{GA_u}{GA_d};\ \text{where } GA_u = \Psi(-\phi_b, \pi/2, 3\pi/2) \tag{4}$$

In addition to left/right ambiguities, there are Doppler ambiguities. In general, the antenna pattern must provide the necessary isolation between a point in the desired scene and these ambiguous points. The third measure of antenna performance is how well it eliminates Doppler ambiguities. Let f_{prf} be the pulse repetition frequency. Then the Doppler shift must be less than $f_d = 2v\sin(\theta)(f/c) = f_{prf}/2$.

We let $f_{prf} = v \cdot k / \Delta x$ from equation (10) and let $k = 1.6$ as a reasonable sampling rate. Thus, this measure may be determined solely from the antenna pattern. The angle where folding begins is $\theta_{dop}(f) = \sin^{-1}\left(f_{prf} \cdot c / (4 \cdot v \cdot f)\right)$. The gain-aperture product over these Doppler ambiguous angles is:

$$\begin{aligned} GA_{dop} = {} & \Psi\left(\phi, \theta_{dop}(f), \pi/2\right) + \Psi\left(-\phi, \pi/2, \pi - \theta_{dop}(f)\right) + \Psi\left(-\phi, \pi + \theta_{dop}(f), 3\pi/2\right) \\ & + \Psi\left(\phi, 3\pi/2, 2\pi - \theta_{dop}(f)\right) \end{aligned} \tag{5}$$

The Doppler ambiguity ratio is then given by the ratio of the gain-aperture in the Doppler ambiguous angles, to the gain-aperture over the desired integration angle:

$$A_{dop} = GA_{dop} / \ \Psi(\phi_b, -\theta_L(f)/\ 2,\ \theta_L(f)/\ 2) \tag{6}$$

4.0 ANTENNA IMPACT ON CROSS-RANGE RESOLUTION

Another antenna performance metric is its potential resolution—the resolution it is capable of producing for a stripmap SAR. We avoid direct calculation of the spatial impulse response width for simplicity. Instead, we present here an approximate calculation that serves as a simple way of comparing various antennas from data sheet values. If θ_e is the effective angle subtended by the synthetic aperture at the pixel being imaged, or in other words, an effective integration angle, then resolution, in the narrow-band uniform aperture weighting case, is given by

$$\Delta x(f) = \frac{c/f}{4\sin(\theta_e(f)/2)}. \tag{7}$$

One might simply average the resolution across the frequency spectrum to provide an approximate resolution. A better approach is to define a weighted average as follows. Define an effective scene tangent, a_e, as the effective synthetic aperture length divided by R_{sb}, the minimum slant range:

$$a_e(f) = \frac{1}{R_{sb}} \int_{-l/2}^{l/2} \frac{\left|G_{\phi_b}(f, \theta(x))\right|^2}{\max\limits_{\theta_m}\left(\left|G_{\phi_b}(f, \theta_m)\right|^2\right)} \left(\frac{R_{sb}}{R_s}\right)^4 dx \underset{l \to \infty}{=} \int_{-\pi/2}^{\pi/2} \frac{\left|G_{\phi_b}(f, \theta)\right|^2}{\max\limits_{\theta_m}\left(\left|G_{\phi_b}(f, \theta_m)\right|^2\right)} \cos^2(\theta)\, d\theta. \tag{8}$$

This allows an *effective integration angle* to be defined by

$$\theta_e(f) = 2 \cdot \tan^{-1}\left(a_e(f)/2\right). \tag{9}$$

Now θ_e can be substituted into (7). Since θ_e is frequency dependent, it is appropriate to average the denominator over the frequency range used with appropriate weighting to reflect the antenna's gain-squared as well

as the λ^2 factor (i.e. $(c/f)^2$) from (1), the radar energy equation. The resulting expression is:

$$\Delta x = \frac{c\int_{f_1}^{f_2} \frac{1}{f^2} \max_{\theta_m}\left(\left|G_{\phi_b}(f,\theta_m)\right|^2\right) df}{4\int_{f_1}^{f_2} \left(\frac{1}{f} \max_{\theta_m}\left(\left|G_{\phi_b}(f,\theta_m)\right|^2\right) \sin\left[\tan^{-1}\left(\frac{1}{2\max_{\theta_m}\left(\left|G_{\phi_b}(f,\theta_m)\right|^2\right)} \cdot \int_{-\pi/2}^{\pi/2} \left|G_{\phi_b}(f,\theta)\right|^2 \cos^2(\theta) d\theta\right)\right]\right) df}. \quad (10)$$

5.0 ANTENNA IMPACT ON MISMATCH LOSS

In practice, desired spatial impulse response and SNR are in conflict and must be traded off. Sensitivity may be measured against that achievable by a matched filter. One measure of the impact of the antenna on this tradeoff is called the mismatch loss. It is the ratio between the SNR obtained with a matched filter, and the SNR obtained with a mismatched filter that provides a desired spatial impulse response in the image.

Let $W_t(f)$ be a window describing the transmitted waveform spectrum (e.g. the square root of a Hamming window), $\eta_0 = 377\Omega$ free space impedance, Z_0 the system impedance, $H_t(f,\theta) = \sqrt{\eta_0 \cdot G(f,\theta)/(4\pi Z_0)}$ the volts/meter per volt transfer function of the transmit antenna, $H_r(f,\theta) = -j \cdot Z_0 \cdot H_t(f,\theta) \cdot c/(f \cdot \eta_0)$ the volts per volts/meter receive antenna transfer function [2], $T(f,\theta)$ the transfer function of the target (i.e., 1 for a point target), $N_e(f,\theta)$ all noise in the environment, $N_r(f,\theta)$ noise in the receiver, and $W_r(f,\theta)$ the filter in the receiver. We will assume that $H_t(\theta,f)$ has been normalized to rotate about its phase center. This is usually accomplished by the following procedure, where IFT is the inverse Fourier transform. Let $h_0(t,\theta) = RE\{IFT[W_t(f) H_t(f,\theta) \cdot |H_t(f,0)|/(|H_t(f,\theta)| \cdot H_t(f,0))]\}$. Let $t_p(\theta) = \arg\max_t (h(t,\theta) \otimes h(t,0))$, the time to the peak correlation between the response at $\theta = 0$ and response at other angles. Let $t_s(\theta) = a_0 + a_1 \cos(\theta + a2)$, a lever-arm time correction. Let $a_0, a_1,$ and a_2 be the solution to the weighted least squares minimization of $\int_{-\theta_L}^{\theta_L} \left| t_s(\theta) - t_p(\theta) \right|^2 \cos(\theta)\, d\theta$. Now, $H_t(\theta,f) = H_{\text{measured}}(\theta,f) \cdot \exp(-j \cdot (t_s(\theta) f))$.

The effective distribution of the signal and noise voltage received—taking into account power-vs-range via the $\cos(\theta)$ term derived in Equation (2)—is,

$$\begin{aligned} T_s(f,\theta) &= [[(W_t(f) \cdot H_t(f,\theta) \cdot T(f,\theta)\cos(\theta) + N_e(f,\theta)) \cdot H_r(f,\theta)] + N_r(f)] \cdot W_r(f,\theta) \\ &\approx [[(W_t(f) \cdot T(f,\theta)\cos(\theta)) \cdot G(f,\theta) \cdot jc/(4\pi f)] + N_r(f)] \cdot W_r(f,\theta) \end{aligned}. \quad (11)$$

The matched filter is $W_r(f,\theta) = [W_t(f) \cdot \cos(\theta) \cdot G(f,\theta) \cdot j \cdot c/(4\pi f)]^*$ when receiver noise limited. The inverse filter is $W_r(f,\theta) = Wd(f,\theta)/[W_t(f) \cdot \cos(\theta) \cdot G(f,\theta) \cdot j \cdot c/(4\pi f)]$ where W_d is a window that produces the desired image impulse response. Following a derivation similar to Equation 3, we find the mismatch loss power:

$$Lmm = \frac{\int_{f_1}^{f_2} \int_{-\theta_L(f)/2}^{\theta_L(f)/2} |W_r(f,\theta)|^2 df\, d\theta \cdot \int_{f_1}^{f_2} \int_{-\theta_L(f)/2}^{\theta_L(f)/2} \left| W_t(f) \cdot G(f,\theta) \cdot \frac{\cos(\theta)}{f} \right|^2 df\, d\theta}{\left| \int_{f_1}^{f_2} \int_{-\theta_L(f)/2}^{\theta_L(f)/2} W_r(f,\theta) \cdot W_t(f) \cdot G(f,\theta) \cdot \frac{\cos(\theta)}{f} d\theta\, df \right|^2}. \quad (12)$$

Here, W_r is the *inverse* filter. We find that equation (12) is minimized when $\theta_L(f) \approx 1.6\theta_e(f)$ from equation (9).

6.0 LOSS FROM VARIATION OFF BORESITE

In most of the previous measures, we assumed that desired signals focus perfectly by including

equalization in $W_r(f,\theta)$. Typical, SAR is built such that W_r is only optimized for the boresite response, as in $\widetilde{W}_r(f,\theta) = Wd(f,\theta)/\left[W_t(f)\cdot\cos(\theta)\cdot G(f,0)\cdot j\cdot c/(4\pi f)\right]$. Another important metric is the loss—relative to ideal angle-variant equalization—due to changes relative to boresite. This metric is the ratio between the two cases.

$$L_{OBV}(\phi_b) = \frac{\left|\int_{f_1}^{f_2}\int_{-\theta_L(f)/2}^{\theta_L(f)/2} \widetilde{W}_r(f,\theta)\cdot W_t(f)\cdot G_{\phi_b}(f,\theta)\cdot\frac{\cos(\theta)}{f}\,d\theta\,df\right|^2 \cdot \int_{f_1}^{f_2}\int_{-\theta_L(f)/2}^{\theta_L(f)/2}\left|W_r(f,\theta)\right|^2 df\,d\theta}{\left|\int_{f_1}^{f_2}\int_{-\theta_L(f)/2}^{\theta_L(f)/2} W_r(f,\theta)\cdot W_t(f)\cdot G_{\phi_b}(f,\theta)\cdot\frac{\cos(\theta)}{f}\,d\theta\,df\right|^2 \cdot \int_{f_1}^{f_2}\int_{-\theta_L(f)/2}^{\theta_L(f)/2}\left|\widetilde{W}_r(f,\theta)\right|^2 df\,d\theta}. \quad (13)$$

7.0 POLARIMETRIC MEASURES

A common occurrence in the cross-pol response of an antenna is a phase reversal about the boresite. This phase produces an artifact in the imagery. A co-pol target, although appearing as a null in the cross-pol image at the target pixel, appears as a pair of targets—one to the left and one to the right (in x) of the true target pixel. A metric that indicates the coupling of co-pol responses into the cross-pol image is to integrate the absolute value of the co-pol and cross-pol responses, and take their ratio. Equation (14) shows this metric, where the *hv* super-script indicates the V-pol antenna response to an incident H-pol plane wave.

$$A_{hv} = \frac{\left(\int_{f_1}^{f_2}\int_{-\theta_L(f)/2}^{\theta_L(f)/2}\left|W_r(f,0)\cdot W_t(f)\cdot G_{\phi_b}^{hv}(f,\theta)\cdot\frac{\cos(\theta)}{f}\right|d\theta\,df\right)^2}{\left(\int_{f_1}^{f_2}\int_{-\theta_L(f)/2}^{\theta_L(f)/2}\left|W_r(f,0)\cdot W_t(f)\cdot G_{\phi_b}^{hh}(f,\theta)\cdot\frac{\cos(\theta)}{f}\right|d\theta\,df\right)^2}. \quad (14)$$

Another metric is the orthogonality between the two antenna ports. Polarimetric transformations are lossless only when the antenna ports are polarimetrically orthogonal. This metric provides a measure of the losses—post-polarimetric calibration—due to the ports not being orthogonal. Where $X = h$ or v and the *h*-pol field produced from the "vertical" transmit port is given by the transfer function H_t^{vh}, the metric becomes

$$L_{PO} = \frac{\int_{f_1}^{f_2}\int_{-\theta_L(f)/2}^{\theta_L(f)/2}\left|\hat{e}_{v_{\phi_b}}(f,\theta)\bullet\hat{e}_{h_{\phi_b}}(f,\theta)\right|^2\left|W_t(f)\cdot G_{\phi_b}(f,\theta)\cdot\frac{\cos(\theta)}{f}\right|^2 d\theta\,df}{\int_{f_1}^{f_2}\int_{-\theta_L(f)/2}^{\theta_L(f)/2}\left|W_t(f)\cdot G_{\phi_b}(f,\theta)\cdot\frac{\cos(\theta)}{f}\right|^2 d\theta\,df} \text{ and } \hat{e}_X = \frac{H_t^{Xh}\cdot\hat{i} + H_t^{Xv}\cdot\hat{j}}{\left|H_t^{Xh}\cdot\hat{i} + H_t^{Xv}\cdot\hat{j}\right|}. \quad (15)$$

8.0 RESULTS

In this section, we evaluate the six measures of merit—effective gain-aperture product, achievable cross-range resolution, mismatch loss, and ambiguity ratio—for two example antennas under various conditions. The first example antenna is a mathematical idealization designed to be suitable for achieving roughly 0.5 meter cross-range resolution, using the band of 150 to 550 MHz. It is based upon the pattern of a cosine-tapered line source, and its gain is proportional to frequency. The equation for its pattern as a function of azimuth angle and frequency, with $L = 1.33$m is

$$G_i(f,\theta) = \frac{2\pi f}{365.5\cdot 10^6}\left(\frac{\cos(\pi L\sin(\theta)(f/c))}{1-(2L\sin(\theta)(f/c))^2}\right)^2. \quad (16)$$

The second example is a circles array designed and built by BATC under contract to the Defense Advanced Research Projects Agency (DARPA). It was designed to meet specifications consistent with the idealized model described above, for dual-polarization and to be mounted onto the Global Hawk UAV. The pattern at HH polarization of one particular great-circle cut is shown in Figure 1.

In doing the calculations, we assumed the following system parameters: frequency band = 150–550 MHz, and $_t(f) = 1/(f_2 - f_1)$, $W_d(f,\theta)$ = 30dB Taylor in each direction. Table 1 summarizes the results. We set the integration limits to $\theta_L(f) = 1.6\theta_e(f)$. These metrics reveal much about the antennas which would be difficult, if

not impossible, to determine by inspection of their patterns alone. A comparison of the effective gain-aperture products of the ideal pattern versus the circles array is of significance to a SAR system designer who is trying to achieve a required polarization purity and SNR. (Where "noise" can be both additive and multiplicative as in the case of ambiguities.) The circles array falls significantly short of that of the ideal pattern; though the ideal pattern may be unrealistic and as far as we know—it was simply a convenient test case.

TABLE 1. RESULTS FOR EXAMPLE ANTENNAS

Measure	Symbol	Ideal	Circles HH	Circles VV
Gain-Aperture Product	GA_d	15.5 m^2	3.7 m^2	8.6 m^2
Potential Cross-Range Resolution	Δx	0.8 m	1.07 m	0.95 m
Mismatch Loss	L_{mm}	1.7 dB	4.6 dB	2.6 dB
Left/Right Ambiguity Ratio	A_{LR}		–20.0 dB	–25.5 dB
Doppler Ambiguity Ratio	A_{dop}	–14.1 dB	–12.4 dB	–13.7 dB
Polarimetric Coupling Ambiguity	A_{hv} , A_{vh}		–9.1 dB	–13.4 dB
Loss From Off-Boresite Variation	L_{OBV}	0. dB	4.3 dB	2.1 dB
Loss From Polarimetric Orthogonality	L_{PO}		0.2 dB	0.2 dB

9.0 CONCLUSIONS

In this paper, we have defined eight antenna measures of merit, or metrics, to apply to ultrawide SAR, where the antenna must perform over very large angles and bandwidths. These measures, which are similar to common system performance measures, may be computed from measured antenna patterns. Other than the antenna pattern, they depend only on a choice of weighting. Other system parameters, such as effective antenna integration angle and pulse repetition frequency, may be inferred from the patterns themselves. Therefore, antenna designers who are not necessarily accustomed to SAR issues, can compute these metrics to gain insight into their antenna design as it relates to SAR image quality. We have applied the metrics to two examples, one an idealized mathematical model and one based on actual measurements. The results illustrate the utility of relating both angle and frequency dependence of an antenna design, to SAR sensitivity and image quality.

10.0 REFERENCES

1. E. Ertin, L. Potter, J. McCorkle, "Angle-Variant Polarimetric and Spectral Antenna Compensation Technique For SAR," in *Algorithms for Synthetic Aperture RADAR Imagery*,(Ed Zelnio, ed.), SPIE Vol. 3370, April 1998

2. R. Robertson, M. Morgan, "Ultra-Wideband Impulse Receiving Antenna Design and Evaluation," in *Ultra-Wideband, Short-Pulse Electromagnetics 2*, (ed. L. Carin, L Felsen) NY: Plenum Press, pp. 179-186, 1995

REPORT DOCUMENTATION PAGE

Form Approved
OMB No. 0704-0188

1. AGENCY USE ONLY *(Leave blank)*

2. REPORT DATE
September 1998

3. REPORT TYPE AND DATES COVERED
Final—June 1997–December 1997

4. TITLE AND SUBTITLE
Antenna Measures of Merit for Ultra-Wide Synthetic Aperture Radar

5. FUNDING NUMBERS
DASW01 94 C 0054
DARPA Assignment A-155

6. AUTHOR(S)
Elizabeth Li Ayers, James M. Ralston, R. Paul Maloney, Philip G. Tomlinson, John McCorkle

7. PERFORMING ORGANIZATION NAME(S) AND ADDRESS(ES)
Institute for Defense Analyses
1801 N. Beauregard St.
Alexandria, VA 22311-1772

8. PERFORMING ORGANIZATION REPORT NUMBER
IDA Document D-2200

9. SPONSORING/MONITORING AGENCY NAME(S) AND ADDRESS(ES)
Defense Advanced Research Projects Agency
Information Systems Office
3701 N. Fairfax Drive
Arlington, VA 22210

10. SPONSORING/MONITORING AGENCY REPORT NUMBER

11. SUPPLEMENTARY NOTES

12a. DISTRIBUTION/AVAILABILITY STATEMENT
Approved for public release; distribution unlimited.

12b. DISTRIBUTION CODE

13. ABSTRACT *(Maximum 180 words)*
This paper addresses the issue of how to characterize an antenna's performance in a SAR system—particularly in ultra-wide-bandwidth and/or ultra-wide-angle (UWB/A) SAR—based on simple gain-magnitude versus frequency and angle measurements provided in data sheets. We present eight measures of merit. As illustrative examples, we compare an ideal mathematical model to measurements of an actual antenna designed to perform UWB/A SAR over up to 65-degree integration angles and over a 150- to 550-MHz frequency band.

14. SUBJECT TERMS
Ultra-Wideband Radar Antennas

15. NUMBER OF PAGES
8

16. PRICE CODE

17. SECURITY CLASSIFICATION OF REPORT	18. SECURITY CLASSIFICATION OF THIS PAGE	19. SECURITY CLASSIFICATION OF ABSTRACT	20. LIMITATION OF ABSTRACT
UNCLASSIFIED	UNCLASSIFIED	UNCLASSIFIED	SAR

NSN 7540-01-280-5500

Standard Form 298 (Rev. 2-89)
Prescribed by ANSI Std. Z39-18
298-102